Flow Induced Vibration of Tube Bundles Subjected to Single- and Two-Phase Cross-Flow

W. Mann [a] and F. Mayinger [b]

[a]Lehrstuhl A für Thermodynamik, Technische Universität München,
80290 München, Germany,
Tel.:+49-89-2105-3246, Fax: +49-89-2105-3451
E-Mail: mann@thermo-a.mw.tu-muenchen.de

[b]Lehrstuhl A für Thermodynamik, Technische Universität München,
80290 München, Germany,
Tel.:+49-89-2105-3436, Fax: +49-89-2105-3451
E-Mail: may@thermo-a.mw.tu-muenchen.de

The vibration behaviour of a normal square tube bundle ($d = 22mm$, $p/d = 1.5$) subjected to single- and two-phase cross-flow is studied. The experiments are done with all tubes flexible. Freon12 is used as a working fluid. Void fraction fluctuations inside of the flexible tube bundle are measured using two optical probes. The fluidelastic instability mechanism at two-phase flow conditions is described.

Nomenclature

A	$[m^2]$	flow area without tube bundle, $A = 100 \times 132\ mm^2$
A_{gap}	$[m^2]$	flow area in the gap, $A_{gap} = 4 \times 11 \times 100\ mm^2$
d	$[m]$	tube diameter, $d = 22mm$
f	$[Hz]$	tube frequency
f_0	$[Hz]$	natural frequency
K	$[-]$	instability factor
M_d	$[-]$	mass-damping parameter
m	$[kg/m]$	mass per unit length
$\dot{m}$	$[kg/(m^2 \cdot s)]$	mass flux
n	$[-]$	exponent
p	$[Pa]$	pressure
p/d	$[-]$	pitch to diameter ratio
RMS	$[m]$	Root Mean Square value of the tube displacement
T	$[^\circ C]$	temperature
u	$[m/s]$	velocity
x	$[m]$	amplitude of the tube
$\alpha_{l,i}$	$[\%]$	local void fraction of the optical probe at position i
$\bar{\alpha}_{l,j}$	$[\%]$	average value of the local void fractions along the whole length of the transverse distance
η	$[Pa \cdot s]$	dynamic viscosity
ξ	$[-]$	total damping
ϱ	$[kg/m^3]$	density
σ	$[N/m]$	surface tension

Subscripts

a	added
$crit$	critical
e	equivalent
f	fluid
g	gas
gap	gap
i	position of the optical probe in the tube bundle
j	number of the optical probe $j = 1$, optical probe 1 $j = 2$, optical probe 2
l	liquid
m	mixture
red	reduced
s	structural
t	tube

1. Introduction

Two-phase cross-flow exists in many shell-and tube-heat exchangers, such as condensers, evaporators, reboilers and nuclear steam generators. Optimum component performance often requires high flow velocities, while reduced structural support is desirable in order to minimize pressure drop and manufacturing costs. High flow velocities and reduced structural support can lead to severe flow induced vibration, which in turn may cause tube failures by fatigue or by fretting-wear. It is essential to avoid such costly tube failures. This can be achieved by a careful analysis of flow-induced vibration, preferably already at the design stage. Therefore, we must understand vibration excitation mechanisms in tube bundles subjected to two-phase cross-flow.

Up to now most of the experimental investigations were performed with air and water, i.e. *Pettigrew et al. [12][13][14][15], Hara et al. [7][8][9][10], Carlucci et al. [2][3], Remy [16]* and *Joo and Dhir [11]*. Physical properties of the air-water mixture are quite different to the steam-water mixture used i.e. in nuclear steam generators *Gay et al. [5]*, see Tab.1. In order to achieve similar physical properties to steam-water mixtures and to reduce costs we used freon 12 (see Tab.1).

Vibration excitation mechanisms caused by two-phase flow can be understood much better, if we can get more information about the temporal and local variation of the void fraction. Therefore, void fraction fluctuations were measured inside of a normal square tube bundle.

2. Experimental Considerations

2.1. Two - phase - loop

The experimental loop was run at pressure of $10 \cdot 10^5 Pa$ in order to get nearly the same density ratio as a steam-water mixture at $70 \cdot 10^5 Pa$ (Tab.1). The tube bundle was subjected to single- and two-phase cross-flow at mass flux $963 \leq \dot{m}_{gap} \leq 1443\ kg/(m^2 \cdot s)$ and volumetric void fraction $0 - 70\%$.

Table 1
Physical properties of air-water, steam-water *Gay et al.[5]* and freon 12.

	air water	steam water	freon12
p $[\cdot 10^5 Pa]$	1	70	10
p/p_{crit} $[-]$	–	0.32	0.23
T $[°C]$	20	286	41.0
ϱ_l $[kg/m^3]$	997	740	1245
ϱ_g $[kg/m^3]$	1.21	37	57
ϱ_l/ϱ_g $[-]$	824	20	22
η_l $[\cdot 10^{-6}\ Pa \cdot s]$	1001	94	193
η_g $[\cdot 10^{-6}\ Pa \cdot s]$	18	19	14
η_l/η_g $[-]$	55	5	14
σ $[\cdot 10^{-3}\ N/m]$	72.7	17.5	6.7

2.2. Test section

Experiments were performed on a normal square tube bundle with all tubes flexible. The pitch to diameter ratio of this tube bundle was 1.5. It consists of 5 tube-rows with 3 tubes in each row. The tubes were cantilevered to permit realistic tube frequencies $(10 - 60\ Hz)$ in a small flow area $(A = 100\ mm \times 132\ mm)$ and to maintain well defined tube support conditions. The natural frequency f_0 of the tubes was $22.5\ Hz$. Stainless steel tubes of $22\ mm$ diameter were used. Half sized tubes were installed on each side of the flow channel to minimize wall effects.

The amplitudes were measured in lift- and drag-direction by inductive displacement transducers. These displacement transducers were mounted in the opposite side wall of the flow channel at a distance of $1\ mm$ to the front-side of the oscillating tube. With this measurement technique we achieved an amplitude resolution of

10 μm. Local variations of the void fraction inside the tube bundle were measured by two optical probes (Fig.1). The optical probes were placed behind the first and the second row of the flexible normal square arrangement. With a transverse equipment it was possible to position each optical probe every three millimeter in axial direction. The optical probes determine either gas or liquid. From the voltage signal the local void fraction $\alpha_{l,i}$ at each position i was calculated by integrating the periods of gas. This value was then related to the whole period t (Eq.1).

$$\alpha_{l,i} = \frac{\int_0^t \Delta t_g}{t} \qquad (1)$$

i=1 .. 23, number of the position of the optical probe

An average value of the local void fractions $\alpha_{l,i}$ along the whole length of the transverse distance was also calculated for each optical probe.

$$\bar{\alpha}_{l,j} = \frac{1}{n} \sum_{i=1}^{n} \alpha_{l,i} \qquad (2)$$

$n = 23$
$j = 1, 2$
$j = 1,$ opt. probe 1
$j = 2,$ opt. probe 2

The mean value of the optical probe 2 ($\bar{\alpha}_{l,2}$) was then used as an representive value for the void fraction inside of the tube bundle.

3. Vibration Response Behaviour

3.1. Vibration behaviour

3.1.1. Influence of void fraction

Fig.2 reproduces a typical vibration response with increasing void fraction. A reduced amplitude is calculated by Eq.3

$$red.\ amplitude = \frac{2 \cdot RMS}{d} \cdot 100\ [\%]. \qquad (3)$$

The main characteristics are:

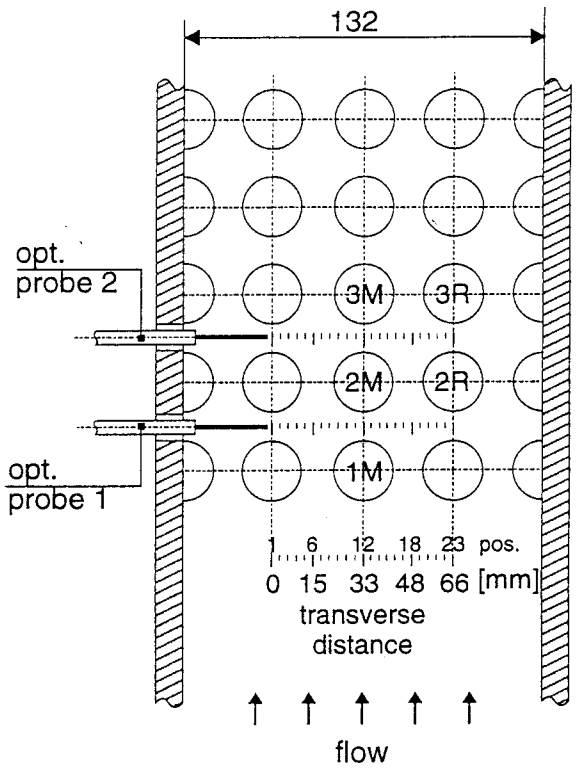

Figure 1. Location of the optical probes and tubes 1M, 2M, 2R, 3M and 3R, which amplitudes were measured at the normal square tube bundle

1. At the transition from single- to two-phase flow, bubbles, up to void fractions $\bar{\alpha}_{l,2}$ of 13%, reduce the amplitude.

2. Increasing the void fraction leads to a linear increase of the vibration amplitude in drag- and lift-direction.

3. At certain void fractions, (Fig.2, $\bar{\alpha}_{l,2}$ = 64%) the vibration amplitude suddenly increases. These operating points are used for characterizing the threshold of fluidelastic instability.

4. The vibration behaviour is similar for all tubes although there are differences in the magnitude of the amplitude at single-phase flow and at fluidelastic instability.

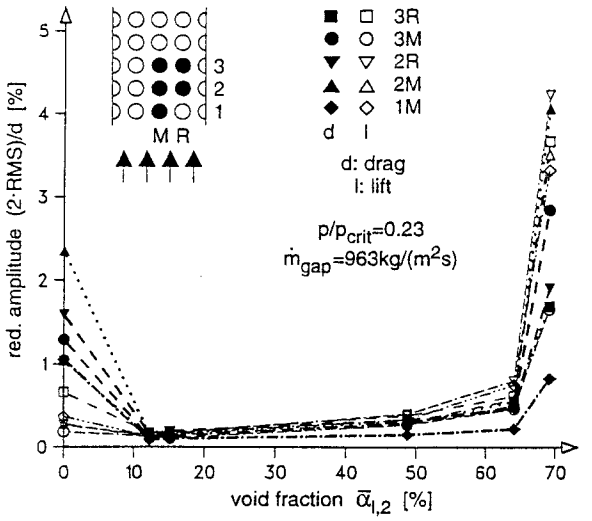

Figure 2. Reduced amplitude versus void fraction, influence of void fraction, $p/d = 1.5$, $f_0 = 22.5\ Hz$.

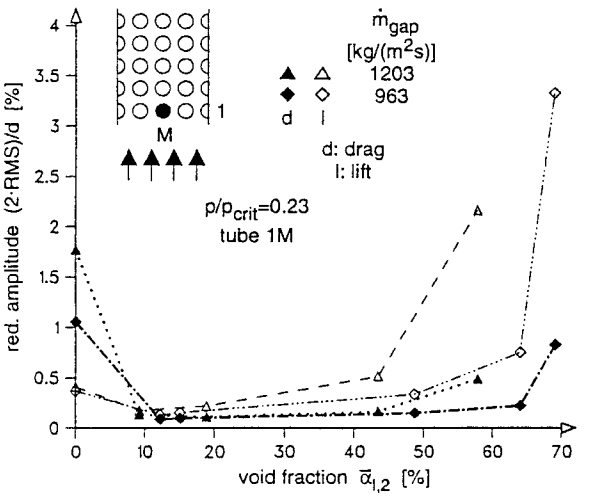

Figure 3. Reduced amplitude versus void fraction, influence of mass flux, $p/d = 1.5$, $f_0 = 22.5\ Hz$.

3.1.2. Influence of mass flux

There are two main effects depending on the mass flux (Fig.3).

1. With increasing mass flux fluidelastic instability occurs at lower void fractions.
2. At constant void fractions amplitudes increase with increasing mass flux.

3.1.3. Influence of tube row

Considering the whole series of experiments, there is no tube row vibrating much more, than any of the other tube rows (i.e.Fig.2).

3.2. Frequency response

The variation of void fraction has the most important influence on the frequency spectra. Changing the mass flux $\dot{m}_{gap}$ at constant void fraction does not influence the tube frequency very much. Typical power spectra with increasing void fraction and constant mass flux and pressure are shown in Fig.4.

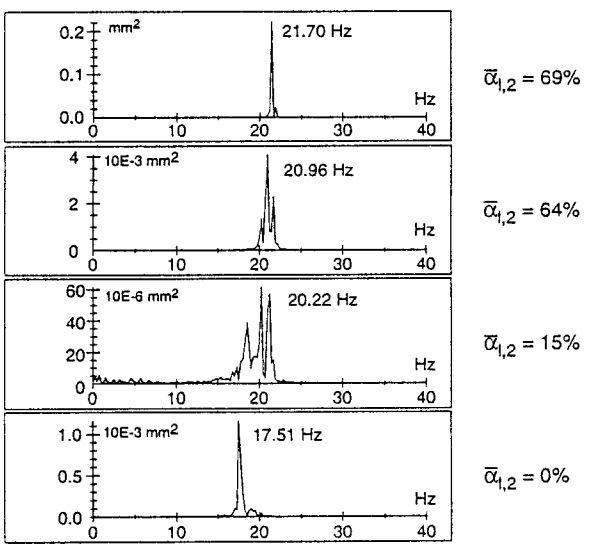

Figure 4. Frequency response, influence of void fraction, tube 1M, lift, $p/p_{crit} = 0.23$, $\dot{m}_{gap} = 963\ kg/(m^2 \cdot s)$, $p/d = 1.5$, $f_0 = 22.5\ Hz$.

The main aspects are:

1. The tube frequency is changing from $17.51 Hz$ to $21.70 Hz$ with increasing void fraction.
2. At liquid flow the power spectrum contains a narrow-band peak. Between void fractions $\bar{\alpha}_{l,2} = 15\%$ and $\bar{\alpha}_{l,2} = 64\%$ the frequencies occur in a broad band.

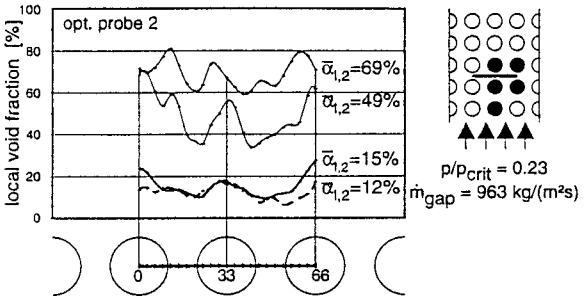

Figure 5. Influence of the void fraction on the phase distribution between the second and the third tube row, optical probe 2, $p/d = 1.5$, $f_0 = 22.5\ Hz$.

3. At a further increase of the void fraction up to $\bar{\alpha}_{l,2} = 69\%$ the response changes from a relatively broad-band spectrum to a narrow-band spectrum.

3.3. Local void fraction

The phase distribution between the second and the third row with increasing void fraction is shown in Fig.5.
The main features are as follows:

1. Most of the steam is located in the wake region.

2. The difference between the local void fraction in the wake region and the one in the stream through the gap rises with increasing void fraction $\bar{\alpha}_{l,2}$.

3. At the highest void fraction of $\bar{\alpha}_{l,2} = 69\%$, where fluidelastic instability occurs (see Fig.2) the maxima are not exactly behind the tubes, but close to the separation points of the tubes.

An increase of the mass flux from $988 kg/(m^2 s)$ to $1205 kg/(m^2 s)$ (Fig.6) at nearly constant void fraction has only a small influence on the shape of the phase distribution.

The difference in the phase distribution behind the first and second tube row is weak, see Fig.7. At void fractions $\bar{\alpha}_{l,2} = 15\%$ and $\bar{\alpha}_{l,2} = 49\%$ the shape of the local void fraction is very similar. Merely at high void fractions of $\bar{\alpha}_{l,2} = 49\%$ the

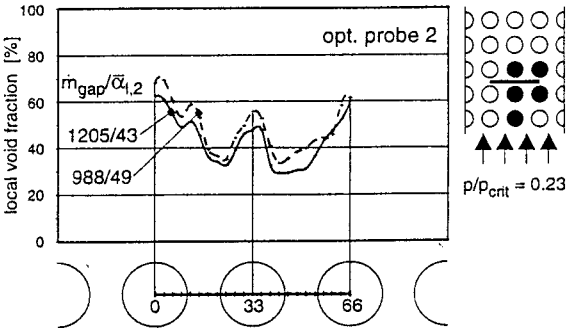

Figure 6. Influence of the mass flux on the phase distribution between the second and the third tube row, probe 2, $p/d = 1.5$, $f_0 = 22.5\ Hz$.

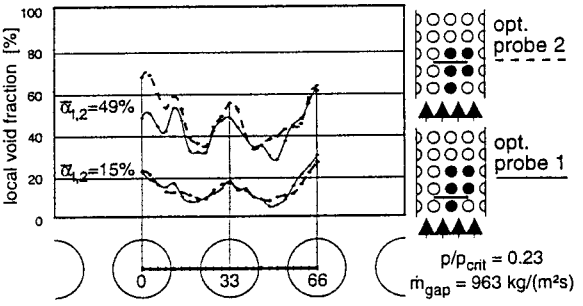

Figure 7. Influence of the tube row on the phase distribution between the tube rows 1/2 and 2/3, $p/d = 1.5$, $f_0 = 22.5\ Hz$.

local void fraction behind the second row is a bit higher, especially in the wake reagion.

4. Fluidelastic Instability

4.1. Fluidelastic instability mechanism

In general, the vibration behaviour of a single tube is influenced by the interaction between the motions of neighbouring tubes and the fluid. *Goyder [6]* illustrates the flow induced vibration problem at single phase flow as a control system presented in Fig.8. The tube produces an output displacement x due to an input force F_3. The force on the tube F_3, caused by the fluid consists of two parts (F_1 and F_2).

F_1 represents the drag force and the turbulent buffeting forces, which are independent of the tube motion. The second part of the force F_2 is due

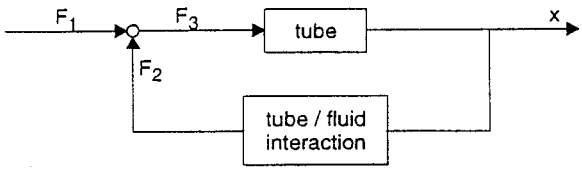

Figure 8. The flow induced vibration problem represented as a control system

to a system, which is correlated with the tube displacement. The feedback path represents the tube/fluid interaction. In this model the feedback causes fluidelastic instability, because, under certain conditions, it reinforces the tube motion. If we want to use this control system not only for the description of the vibration behaviour caused by single-phase flow, but also for the description at two-phase flow conditions, the following question arises:

Is a model with a feedback realistic even in the case of two-phase flow? That means, that the periodic motion of the tube displacement has to be impressed on the random fluctuations of the gas and liquid phase. If the fluctuations of the gas and liquid phase are strongly influenced by the tube motion, the frequency spectra of the optical probes, which are located inside of the tube bundle, will contain the tube frequency. The result is shown in Fig.9, which presents power spectra of the void fraction fluctuations inside of the tube bundle and of the tube 3R at flow conditions, where fluidelastic instability occurs.

Fig.9 indicates that the gas-liquid fluctuations inside the tube bundle are periodic and the corresponding frequency is the same as the frequency of the tube vibration. This is characteristic for a feedback and therefore, a description using a control system as shown in Fig.8 is also appropriate for two-phase flow. At certain flow conditions, depending on void fraction and mass flux the tube frequency can be impressed on the two-phase flow and the periodic hydrodynamic force F_2 increases and reinforces the tube motion.

At flow conditions, where the amplitudes are small, i.e. $\bar{\alpha}_{l,2} = 15\%$, 49% and 64%, $\dot{m}_{gap} = 963 kg/(m^2 s)$, $p/p_{crit} = 0.23$, see Fig.2, the power spectra of the local void fraction are broad band and there is no dominant peak at the tube fre-

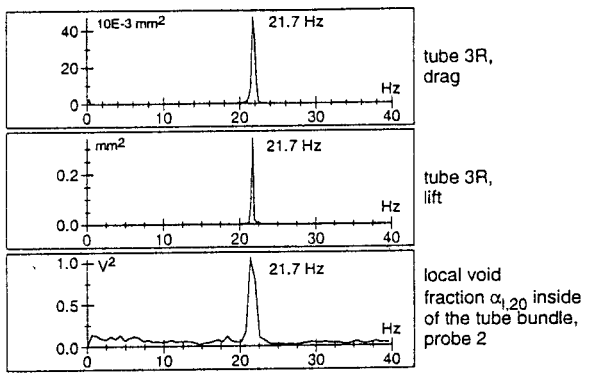

Figure 9. Power spectra at fluidelastic instability ($\bar{\alpha}_{l,2} = 69\%$, $p/p_{crit} = 0.23$, $\dot{m}_{gap} = 963\ kg/(m^2 \cdot s)$), local void fraction $\alpha_{l,20}$ (optical probe 2, pos. 20) and tube 3R in drag and lift, $p/d = 1.5$, $f_0 = 22.5\ Hz$.

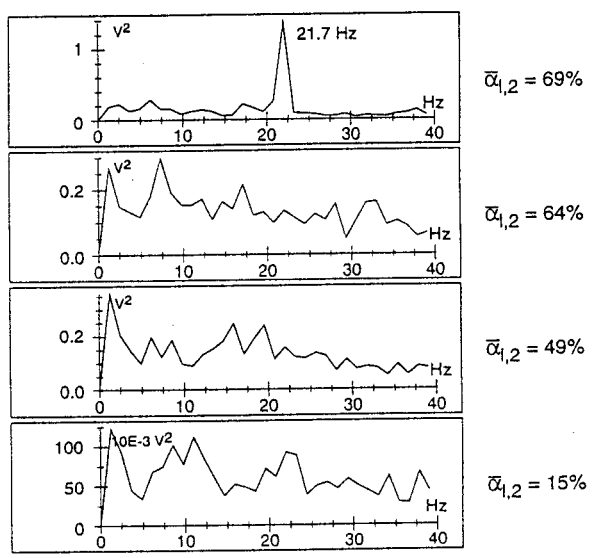

Figure 10. Influence of the void fraction on the frequency spectra of local void fraction (optical probe 2, pos. 20), $p/p_{crit} = 0.23$, $\dot{m}_{gap} = 963\ kg/(m^2 \cdot s)$, $p/d = 1.5$, $f_0 = 22.5\ Hz$.

quency at about 22 Hz (see Fig.10). That indicates, that the feedback between tube motion and gas-liquid fluctuations is weak. As the void fraction is increased up to $\bar{\alpha}_{l,2} = 69\%$ (see Fig.10) a strong feedback between the tube motion and the two-phase flow occures leading to large amplitu-

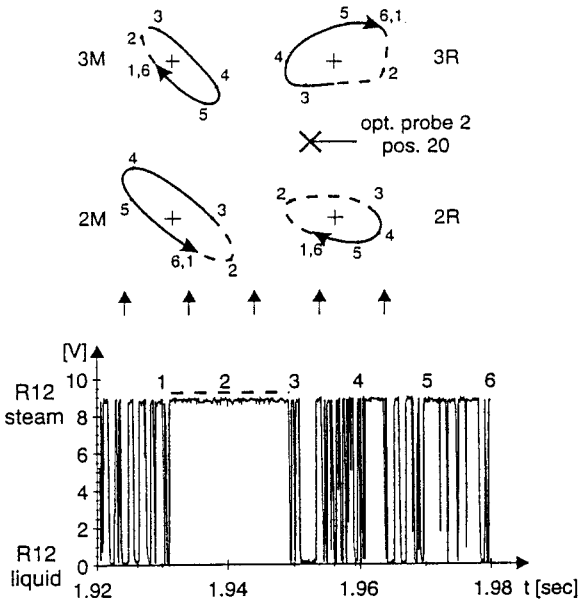

Figure 11. Vibration pattern from tube 2M, 2R, 3M and 3R and the signal from optical probe 2 at position 20 at fluidelastic instability, void fraction $\bar{\alpha}_{l,2} = 69\%$, $p/p_{crit} = 0.23$, $\dot{m}_{gap} = 963\ kg/(m^2 \cdot s)$, $p/d = 1.5$, $f_0 = 22.5\ Hz$.

des.

To gain a better impression about the interaction between the tube vibration and the fluctuations of the gas-liquid phase a cycle of the movement of the tubes 2M, 2R, 3M and 3R and the signal of the optical probe 2 at position 20 is presented in Fig.11.

From 1 to 3 the tubes of the second row 2M and 2R are moving together and the cross section between those tubes becomes small. At the same time downstream the tubes 3M and 3R move away from each other. This periodic reduction and enlargement of the cross channel is impressed on the gas-liquid mixture. The corresponding signal of the optical probe shows that in the case of a small flow channel between tube 2M and 2R (1-3) the gas phase streams through this small channel because of small inertia. If the flow channel between tubes 2M and 2R is enlarged, the liquid phase streams downstream and pushes tubes 3M and 3R. This is more clearly understood, when studying the vibration pattern during time steps 4 and 5 of tube 3R.

4.2. Fluidelastic instability results

Fluidelastic instability may be formulated in terms of a dimensionless flow velocity, u_{red} Eq.4, and a dimensionless mass-damping parameter, M_d Eq.5, *Connors [4]*

$$u_{red} = \frac{u_{crit,gap}}{f \cdot d} \tag{4}$$

$$M_d = \frac{2\pi\xi \cdot m}{\varrho_m \cdot d^2} \quad . \tag{5}$$

The correlation between those parameters is described by the *Connors* equation (Eq.6)

$$u_{red} = K \cdot (M_d)^n \quad . \tag{6}$$

The variables of the equations 4, 5 and 6 are defined as follows:

$u_{crit,gap}$ $[m/s]$ critical gap velocity

$$u_{crit,gap} = \frac{\dot{m}_{gap}}{\varrho_m}$$

$$\varrho_m = \bar{\alpha}_{l,2} \cdot \varrho_g + (1 - \bar{\alpha}_{l,2}) \cdot \varrho_f$$

Flow conditions ($\dot{m}_{gap}$, $\bar{\alpha}_{l,2}$, p/p_{crit}) can be defined as critical, even though the vibration response is still stable, but if even a small increase of the flow velocity occures, it causes a drastic increase of the vibration response like shown in Fig.2 ($\bar{\alpha}_{l,2} = 69\%$, $\dot{m}_{gap} = 963\ kg/(m^2 \cdot s)$, $p/p_{crit} = 0.23$, critical flow condition).

f $[Hz]$ tube frequency at critical flow condition

d $[m]$ tube diameter

ξ $[-]$ total damping ratio (structural and fluid damping)

Experimental results from *Pettigrew et al. [15]* Fig.12 can be used to estimate fluid damping ($\xi_{f,Fig.12}$). $\xi_s = 0.11\%$ normal square, $\xi_{s,Pett.} = 0.22\%$

$$\xi = \xi_{f,Fig.12} - \xi_{s,Pett.} + \xi_s$$

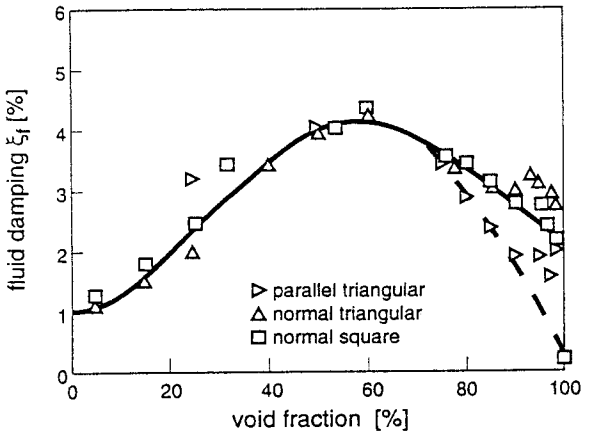

Figure 12. Fluid damping of tube bundles subjected to two-phase cross-flow, *Pettigrew et al.[15]*

m $[kg/m]$ mass per unit length including added mass m_a

$$m = m_t + m_a$$

m_t: mass per unit length of the tube itself
$m_t = 1.602\ kg/m$ normal square;

$$m_a = m_t \cdot \left[\left(\frac{f_0}{f} \right)^2 - 1 \right]$$

$f_0 = 22.5\ Hz$ normal square

All critical flow conditions and calculated values f, ϱ_m, $u_{crit,gap}$, ξ, m_a, m, u_{red}, M_d and K are listed in Tab.2. The values of the instability factor K, mentioned in Tab.2, are based on the exponent n equal to 0.5.

A summary of flow conditions from *Axisa et al. [1], Pettigrew et al. [14]* and own tests leading to fluidelastic instability conditions, which are presented in Fig.13.

A comparison of all available data on fluidelastic instability shows, that only the results of *Pettigrew et al. [14]* are comparable with our results, because only they use geometrical dimensions ($f_0 = 33Hz$, $d = 13mm$, $p/d = 1.47$) and flow conditions ($5 \leq \alpha \leq 99\%$, $50 \leq \dot{m}_{gap} \leq 1200kg/(m^2s)$) similar to ours. At similar mass-damping parameters, values for the reduced velocity tend to be larger. Differences in natural frequency and in the physical properties of the

Table 2
Summary of tests at critical flow conditions

no. [−]	p/p_{crit} [−]	$\dot{m}_{gap}$ $\left[\frac{kg}{(m^2 s)}\right]$	$\bar{\alpha}_{l,2}$ [%]	f $[Hz]$	ϱ_m $\left[\frac{kg}{m^3}\right]$	$u_{crit,gap}$ $\left[\frac{m}{s}\right]$
1	0.23	988.64	64.05	21.7	484.09	2.04
2	0.23	1204.55	43.47	20.7	728.58	1.65
3	0.23	1411.36	31.82	19.3	866.98	1.63

no. [−]	ξ [%]	m_a $\left[\frac{kg}{m}\right]$	m $\left[\frac{kg}{m}\right]$	$\frac{u_{crit,gap}}{f \cdot d}$ [−]	$\frac{2\pi\xi \cdot m}{\varrho_m \cdot d^2}$ [−]	K [−]
1	3.99	0.122	1.724	4.27	1.84	3.15
2	3.44	0.292	1.894	3.62	1.16	3.36
3	2.89	0.577	2.179	3.84	0.94	3.96

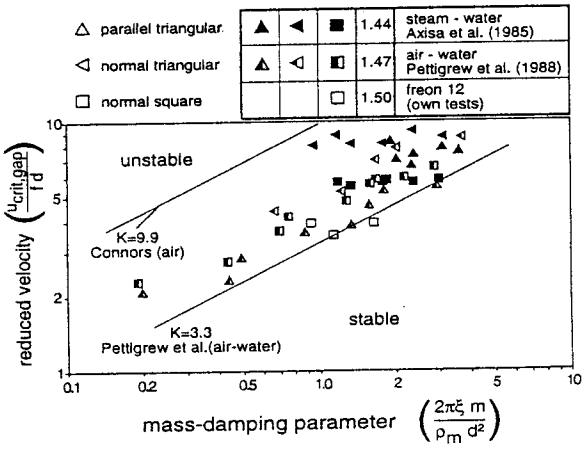

Figure 13. Dimensionless presentation of fluidelastic instability results in two-phase cross-flow. Comparison with results of literature

two-phase mixture could be reasons for this behaviour. For example, density and viscosity of freon12 are quite different from air-water at $20°C$ (see Tab.1). *Axisa et al. [1]* used steam-water and studied fluidelastic instability at higher void fractions, mostly above 85%. Their results are only mentioned in order to give the best possible survey on fluidelastic instability behaviour. They

diverge drastically from our results. As expected *Connors* results from experiments with air show large divergence to our results and to most of other two-phase flow experiments.

5. Concluding Remarks

A tube bundle of normal square configuration and of p/d of 1.5 was subjected to single and two-phase cross-flow conditions. Freon12 was used as a working fluid. The experiments were performed on a tube bundle with all tubes flexible. Void fraction fluctuations inside of the normal square bundle were measured, using two optical probes.

The main results are as follows:

- The mechanism of fluidelastic instability at two-phase cross-flow was identified. At certain flow conditions, depending on void fraction and mass flux the tube motion could be impressed on the fluctuations of the gas and liquid phase and therefore the hydrodynamic force becomes periodic and reinforces the tube motion.

- At the transition from single- to two-phase flow, steam bubbles reduce the hydrodynamic coupling and the amplitudes decrease.

- Results concerning the phase distribution show steam accumulation in the wake of the tubes.

Acknowledgments

The authors greatfully acknowledge financial support for this work by the BMFT (Bundesministerium für Forschung und Technologie, Förderkennzeichen 03E8521A).

REFERENCES

1. **Axisa F., Villard B., Gilbert R.J. and Boheas M.A.:**
8th S.M.I.R.T. Conf., Bruxelles, Belgium, 19-23 Aug., Paper B1/2, 1985.
2. **Carlucci L. N.:**
Trans. of the ASME, J. of Mechanical Design, vol. 102, no. 7, pp. 597-602, 1980.
3. **Carlucci L.N. and Brown J.D.:**
Trans. of the ASME, J. of Vibration, Acustics, Stress and Reliability in Design, vol. 105, pp. 83-89, 1983.
4. **Connors H.J.:**
Int. Symp. on Flow Induced Vibration in Heat Exchangers, ASME Winter Annual Meeting, New York, pp. 42-56, 1970.
5. **Gay N., Decembre P. and Launay J.:**
Int. Symp. of Flow-Induced Vibration and Noise, Winter Annual Meeting of the ASME, Chicago, Illinois, 27 Nov.-2 Dec., vol. 3, pp. 139-158, 1988.
6. **Goyder H.G.H.:**
Vibration in Nuclear Plant, Keswick, England, Paper 1.8, pp. 120-134, 1982.
7. **Hara F.:**
Int. Conf. on Flow Induced Vibrations, Bowness-on-Windermere, England, 12-14 May, Paper E1, pp. 203-210, 1987.
8. **Hara F. and Iijima T.:**
Int. Symp. on Flow-Induced Vibration and Noise, Winter Annual Meeting of the ASME, Chicago, Illinois, 27 Nov.-2 Dec., vol. 2, pp. 63-78, 1988.
9. **Hara F.:**
Int. Conf. on Flow Induced Vibrations, Brighton, U.K., 20-22 May, IMech 1991-6,C416/025, pp. 369-378, 1991.
10. **Hara F., Iijima T. and Nojima T.:**
Trans. of the ASME, J. of Pressure Vessel Technology, vol. 114, no. 11, pp. 444-452, 1992.
11. **Joo Y. and Dhir V.K.:**
Heat Transfer Conf., Atlanta, USA, 8-11 Aug. In: ANS Proc., vol. 7, pp. 137-144, 1993.
12. **Pettigrew M.J. and Gorman D.J.:**
Int. Symp. on Vibration Problems in Industry; Atomic Energy of Canada Limited, Keswick, England, Paper 4.2, pp. 1 - 31, 10-12 April 1973.
13. **Pettigrew M.J. and Gorman D.J.:**
Vibration in Nuclear Plant, Proc. of the British Nuclear Society, Keswick, England, Paper 2.3, pp. 215-232, 1978.
14. **Pettigrew M.J., Tromp J.H., Taylor C.E. and Kim B.S.:**
Int. Symp. of Flow-Induced Vibration and

Noise, Winter Annual Meeting of the ASME, Chicago, Illinois, 27 Nov.-2 Dec., vol. 3, pp. 159-180, 1988.

15. **Pettigrew M.J., Taylor C.E. and Kim B.S.:**
Int. Symp. of Flow-Induced Vibration and Noise, Winter Annual Meeting of the ASME, Chicago, Illinois, 27 Nov.-2 Dec., vol. 2, pp. 79-104, 1988.
16. **Remy F.N.:**
3rd Int. Conf., Keswick, U.K., 11-14 May, Paper 1.9, pp. 135-160, 1982.